NIH Public Access
Author Manuscript
J Invest Dermatol. Author manuscript; available in PMC 2012 August 13.

Published in final edited form as:
J Invest Dermatol. 2009 December ; 129(12): 2818–2822. doi:10.1038/jid.2009.161.

In Vivo Real-Time, Multicolor, Quantum Dot Lymphatic Imaging

Nobuyuki Kosaka[1], **Mikako Ogawa**[1], **Noriko Sato**[1], **Peter L. Choyke**[1], and **Hisataka Kobayashi**[1]

[1]Molecular Imaging Program, Center for Cancer Research, National Cancer Institute, National Institutes of Health, Bethesda, Maryland, USA

Abstract

The lymphatic network is complex and difficult to visualize in real-time *in vivo*. Moreover, the direction of flow within lymphatic networks is often unpredictable especially in areas with well-developed "watershed" or overlapping lymphatics. Herein, we report a method of *in vivo* real-time multicolor lymphatic imaging using cadmium–selenium quantum dots (Qdots) with a fluorescence imaging system that enables the simultaneous visualization of up to five distinct lymphatic basins in real-time. Five visually well-distinguishable carboxyl-Qdots (Qdot 545, 565, 585, 605, and 655) were selected and injected subdermally into mice at five different sites, and serially imaged *in vivo* or *in situ* under surgery with real-time multicolor lymphatic imaging. In all seven mice, *in vivo* lymphatic images successfully distinguished all five lymphatic basins with different colors in realtime. These visualizations of lymph node lasted up to at least 7 days. This method could have a considerable potential in lymphatic research for studying the anatomy and flow within the lymphatic system as well as in some limited clinical settings where real-time visible fluorescence could facilitate procedures under surgery or endoscopy.

INTRODUCTION

The lymphatic network is complex and difficult to visualize *in vivo*. The lymphatics are composed of terminal afferent "collector" ducts that enter the lymphatic sinus in the outer cortex of lymph nodes where innate immunity, a primary defense, can take place. Efferent lymphatic channels emerge from the hilum of the lymph node and generally interconnect with other lymph nodes before finally joining the deep lymphatics, which in turn enter the systemic vascular system through the thoracic duct. Each lymph node can receive lymphatic fluid from multiple afferent lymphatic channels (Hama *et al.*, 2007a, b). Moreover, the direction of flow within lymphatic networks is often unpredictable especially in areas with a well-developed "watershed" or overlapping lymphatics. However, lymphatic flow can be altered during disease states and a method to image the lymphatics is potentially a useful research tool. Several lymphatic imaging methods are now available both pre-clinically and clinically (Barrett *et al.*, 2006; Sharma *et al.*, 2008). These include magnetic resonance, radionuclide and optical methods (Barrett *et al.*, 2006). Optical imaging is unique in that each fluorophore emits a unique spectral wavelength thus permitting simultaneous depiction of multiple lymphatics at the same time, provided that there is minimal overlap of the emission spectra of the fluorophores. Moreover, optical imaging can potentially be

© 2009 The Society for Investigative Dermatology

Correspondence: Dr Hisataka Kobayashi, Molecular Imaging Program, Center for Cancer Research, National Cancer Institute, NIH, Building 10, Room 1B40, MSC1088, Bethesda, Maryland 20892-1088, USA. kobayash@mail.nih.gov.

CONFLICT OF INTEREST

The authors state no conflict of interest.

SUPPLEMENTARY MATERIAL

Supplementary material is linked to the online version of the paper at http://www.nature.com/jid

NIH-PA Author Manuscript
NIH-PA Author Manuscript
NIH-PA Author Manuscript

NIH-PA Author Manuscript

NIH-PA Author Manuscript

NIH-PA Author Manuscript

performed in real-time during surgical procedures. The simultaneous multicolor imaging of five different lymphatic basins using quantum dots (Qdots) or dendrimer-conjugated organic fluorophores has been reported (Kobayashi *et al.*, 2007a, b). However, such imaging requires lengthy spectral unmixing that prevents real-time display. Moreover, the full potential of Qdots were not realized in previous studies; the emission profiles of Qdots are sharp and can be tuned to emit a variety of wavelengths, from a single, lower wavelength excitation light (Goldman *et al.*, 2004). Because the emission profiles are so sharp, it is possible to visualize five different Qdots in the visible range (Figure 1a and b) even with the naked eye. Herein, we report the development of an *in vivo* visible, real-time multicolor lymphatic imaging system using five different Qdots to visualize five distinct lymphatic basins in the neck and axillary region in mice.

RESULTS

In vivo real-time multicolor lymphatic imaging

Among eight commercially available carboxyl-coated Qdots, five cadmium–selenium Qdots (Qdot 545, 565, 585, 605, and 655) were selected in this experiment because of adequate visual color differences (Figure 1a and b). These five Qdots were injected subdermally into five sites as shown in Figure 1c. In all seven mice, *in vivo* images successfully resolved all five lymphatic basins with different colors using real-time and spectral fluorescence imaging (Figure 2a and b). Compared with spectral imaging, real-time multicolor fluorescence imaging did not require image post-processing and thus could be displayed and recorded in real-time (Supplementary Movies S1, S2). The value of multicolor fluorescence imaging is demonstrated in the right superficial neck lymph node of one animal that received drainage from two different afferent lymphatics (arrows in Figure 2b). The upper half of this lymph node exhibited green fluorescence (Qdot 545 from the injection at the chin), whereas the lower half of the node exhibited pale-orange fluorescence (Qdot 585 from the injection in the right ear). These findings became more obvious after tugging on the lymph node in real-time with forceps during *in vivo* imaging (Supplementary Figure S1).

Serial *in vivo* fluorescence imaging

The three mice that were not killed underwent serial *in vivo* fluorescence imaging to investigate the duration of nodal visualization. Imaging sessions took place at 1, 2, and 7 days after injection of Qdots. Compared to the immediate post injection images, day 1 images were considerably weaker (Figure 3) probably because of rapid washing out of the Qdots. However, there was little subsequent loss in the signal enabling imaging at day 7 (Figure 3). Despite this signal loss, all fluorescent emissions from the lymph nodes were clearly seen after stretching the overlying skin when imaging with a video camera as shown in Supplementary Figure S2.

Histological analysis

After removal and *ex vivo* fluorescence imaging, the lymph nodes were evaluated by fluorescence microscopy and immunohistochemistry. On day 0 the Qdots were mainly in the lymphatic sinuses, whereas the lymphoid follicles and lymphatic cords were devoid of Qdots (Figure 4a). The Qdots distributed within the node in an expected distribution: lymph fluid from afferent lymphatic vessels typically enters the subcapsular sinus and then flows through the lateral transverse and medullary sinuses (Willard-Mack, 2006). At high magnification, microscopy showed that the Qdots mostly accumulated within the cytoplasm of histiocytic cells including macrophages and dendritic cells in the lymphatic sinuses adjacent to intranodal channels (Figure 4b and d, Supplementary Figures S3 and S4). The distribution of the Qdots after 7 days was sparser than that of day 0, but still showed the

NIH-PA Author Manuscript

NIH-PA Author Manuscript

NIH-PA Author Manuscript

same pattern (Figure 4c). The majority of the Qdots were taken up by macrophages and dendritic cells whereas a minor fraction was probably washed out within a day.

DISCUSSION

A unique feature of Qdots is that they are so bright that they can be seen with the naked eye. Currently, most of fluorescence lymphatic imaging is performed with near-infrared fluorophores due to its superior penetration of tissue and lower contamination with autofluorescence (Barrett *et al.*, 2006; Frangioni *et al.*, 2007; Sharma *et al.*, 2008). However, because near-infrared fluorescence is invisible to the human eye, it must be imaged with a specially designed near-infrared fluorescence camera (Tanaka *et al.*, 2006), and multicolor imaging is only possible with spectral imaging that allows unmixing of the fluorescence from the background signal (Kobayashi *et al.*, 2007a, b). This process requires a lengthy acquisition time (>2 minutes) and further post processing (requiring another several minutes), and thus, cannot occur in real-time. Our method employs visible-light Qdots, which are so bright that in spite of their lower wavelength, nonetheless penetrate the skin sufficiently for *in vivo* lymphatic imaging. This has advantages for guiding procedures, both pre-clinically and clinically, which often demand real-time interaction with the tissue. For instance, real-time procedures facilitated the detection of sentinel nodes (Supplementary Figures S1 and S2). Although the poor penetration of light limits visualization of nodes to within 2 cm of the skin surface, it is nonetheless helpful to the surgeon to be able to directly visualize the node through the skin in real-time before a sentinel-node resection (Supplementary Movie S1). The deep lymphatic system may not be visualized through the skin due to poor tissue penetration of visible light. This can be partly overcome by the increased brightness of Qdots. Meanwhile real-time imaging allows the direct manipulation (for example, stretching) of the skin to reduce the light path length. It is only necessary to detect a vague signal from deep to the skin, which can be easily seen during open surgery in real-time as shown in Supplementary Movie S2.

There is a limitation to this current imaging system. The color difference between Qdot 605 and 655 is not obvious especially in *in vivo* images (Figures 2b and 3b). However, the color difference among the five Qdots was clearly distinguishable even in *in vivo* imaging with direct visualization without a camera system. This ambiguity can be improved using a camera system with a well-tuned color balance close to naked eyes. Thus, this is unlikely to be a potential impediment to further development of a fluorescence- guided surgical assistance system.

The toxicity of Qdots and their excretion from the body remains another potential limitation for clinical translation (Hardman, 2006; Iga *et al.*, 2007), because most Qdots are composed of heavy metals (for example cadmium and selenium in very small amounts). Robe *et al.* (2008) reported the biodistribution of intradermally injected carboxyl-Qdot 655 in the footpad of the mouse after 24 hours, and found that Qdots were not detected within the organs but could be found in the axillary lymph nodes on the injected side and at the injection site. The author suggested that systemic uptake of intradermally injected Qdots was negligible at 24 hours, so that surgical resection of the injected skin effectively removed residual Qdots from the body. Surface coatings and appropriate sizes may improve the pharmacokinetics and accelerate the removal of the agent from the body thus reducing toxicity (Ballou, 2005; Zhang *et al.*, 2006). Smaller Qdots below 6 nm in diameter are thought to be cleared through the kidney and rapidly excreted into the urine (Choi *et al.*, 2007). Moreover, the dose of Qdots needed for visualizing lymphatics is low and might be below the toxicity threshold in humans, but this issue remains to be investigated.

NIH-PA Author Manuscript

NIH-PA Author Manuscript

NIH-PA Author Manuscript

This real-time multicolor lymphatic imaging method can be applied to any part of the body in mice (Supplementary Figure S5). Moreover, we have recently demonstrated that Qdot-labeled melanoma cells migrate through draining lymphatics identified with fluorescent nanoparticles injected intradermally (Kobayashi *et al.*, 2009). Multicolor cell tracking in the lymphatic system could be another research tool for real-time multicolor lymphatic imaging in cancer research. As the human body size is much larger than the mouse, the use of this method in humans will require further advancements in Qdot technology including minimizing the amount of heavy metals (for example, Cadmium) while retaining the same high efficiency. In addition, improved imaging technologies that enable deeper visualization will be important for clinical translation.

In conclusion, we successfully demonstrated *in vivo* visible real-time multicolor lymphatic imaging in mice using five different Qdots with distinct visible-range emissions. This enabled simultaneous, but separate observation of multiple lymphatic basins in real-time, which persisted up to at least 7 days. This method could have a considerable potential in lymphatic research for studying the anatomy and flow within the lymphatic system as well as in some limited clinical settings where real-time visible fluorescence could facilitate the procedures under surgery or endoscopy.

MATERIALS AND METHODS

Quantum dots

Eight carboxyl quantum dots (Qdot 525 ITK, Qdot 545 ITK, Qdot 565 ITK, Qdot 585 ITK, Qdot 605 ITK, Qdot 655 ITK, and Qdot 705 ITK, Qdot 800 ITK), which have thin coatings and small sizes, were purchased from Invitrogen Co. (Carlsbad, CA).

In vivo real-time multicolor lymphatic imaging

All *in vivo* procedures were carried out in compliance with the Guide for the Care and Use of Laboratory Animal Resources (1996), National Research Council, and approved by the National Cancer Institute Animal Care and Use Committee. Ten-week-old normal athymic female mice were anesthetized through intraperitoneal injection of 1.15mg sodium pentobarbital (Nembutal Sodium Solution, Ovation Pharmaceuticals Inc., Deerfield, IL). Among all available eight carboxyl-Qdots, five cadmium–selenium Qdots (Qdot 545, Qdot 565, Qdot 585, Qdot 605, and Qdot 655) were selected in this experiment because of adequate visual color differences (Figure 1a and b). Seven mice were injected subdermally with 20 μl of each Qdot solution (1.6 μM for Qdot 545, 565, and 585, or 0.8 μM for Qdot 605 and 655) into five different sites: the middle phalanges of the upper extremities (left and right), the ears (left and right), and the chin, as described in Figure 1c. Within 5 minutes after injection, *in vivo* visible multicolor fluorescence imaging was performed with a modified real-time fluorescence imaging system (FluorVivo, INDEC BioSystems, Santa Clara, CA). An excitation band-pass filter of 450–490nm and an emission long-pass filter of 520nm were used. For still images, the real-time video camera was replaced with a commercial-grade digital camera (CoolPix5400, Nikon, Tokyo, Japan) and a digital video camcorder (PV-GS400, Panasonic Corporation of North America, Secaucus, NJ). As a control, *in vivo* spectral fluorescence imaging was performed using a spectral imaging system (Maestro *In Vivo* Imaging System, CRI Inc., Worburn, MA), with 445–490nm excitation band-pass filter and 515nm long-pass emission filter. The tunable filter was automatically stepped in 10nm increments from 500 to 800nm using the same exposure time at each wavelength resulting in one image every 30 seconds. The collected spectral fluorescence images were processed with an unmixing algorithm (Maestro ver2.4, CRi). After obtaining *in vivo* images, four of seven mice were killed, and the lymph nodes were

NIH-PA Author Manuscript

NIH-PA Author Manuscript

NIH-PA Author Manuscript

exposed for *in situ* fluorescence imaging. All removed lymph nodes were also imaged with the same settings as the *in situ* images.

Serial *in vivo* fluorescence imaging

The three mice that were not killed underwent serial *in vivo* fluorescence imaging to investigate the duration of nodal visualization. Imaging sessions took place at 1, 2, and 7 days after injection of Qdots and then the mice were killed and underwent *in situ* and *ex vivo* fluorescence imaging. Imaging protocols were the same as described above.

Histological analysis

After removal and *ex vivo* fluorescence imaging, the right axillary lymph nodes (containing Qdot 655) were fixed with 10% formaldehyde and was evaluated by fluorescence microscopy (Olympus BX61 microscope, Olympus America Inc., Melville, NY) equipped with excitation band-pass filter 530–585nm and emission band-pass filter 605–680 nm. Immunohistochemical staining was also performed with the same lymph node samples. Macrophages/dendritic cells, B cells and T cells were identified by HAM56, anti- CD20, and anti-CD3 antibodies, respectively. The fluorescence signal from Qdot 655 was co-registered with the signals from the immunohistochemical markers. Hematoxylin and eosin staining were also performed and evaluated.

Supplementary Material

Refer to Web version on PubMed Central for supplementary material.

Acknowledgments

This research was supported by the Intramural Research Program of the NIH, National Cancer Institute, Center for Cancer Research.

Abbreviation

Qdot quantum dot

References

Ballou B. Quantum dot surfaces for use *in vivo* and *in vitro*. Curr Top Dev Biol. 2005; 70:103–20. [PubMed: 16338339]

Barrett T, Choyke PL, Kobayashi H. Imaging of the lymphatic system: new horizons. Contrast Media Mol Imaging. 2006; 1:230–45. [PubMed: 17191764]

Choi HS, Liu W, Misra P, Tanaka E, Zimmer JP, Itty Ipe B, et al. Renal clearance of quantum dots. Nat Biotechnol. 2007; 25:1165–70. [PubMed: 17891134]

Frangioni JV, Kim SW, Ohnishi S, Kim S, Bawendi MG. Sentinel lymph node mapping with type-II quantum dots. Methods Mol Biol. 2007; 374:147–59. [PubMed: 17237537]

Goldman ER, Clapp AR, Anderson GP, Uyeda HT, Mauro JM, Medintz IL, et al. Multiplexed toxin analysis using four colors of quantum dot fluororeagents. Anal Chem. 2004; 76:684–8. [PubMed: 14750863]

Hama Y, Koyama Y, Urano Y, Choyke PL, Kobayashi H. Simultaneous two-color spectral fluorescence lymphangiography with near infrared quantum dots to map two lymphatic flows from the breast and the upper extremity. Breast Cancer Res Treat. 2007a; 103:23–8. [PubMed: 17028977]

Hama Y, Koyama Y, Urano Y, Choyke PL, Kobayashi H. Two-color lymphatic mapping using Ig-conjugated near infrared optical probes. J Invest Dermatol. 2007b; 127:2351–6. [PubMed: 17522707]

NIH-PA Author Manuscript

NIH-PA Author Manuscript

NIH-PA Author Manuscript

Hardman R. A toxicologic review of quantum dots: toxicity depends on physicochemical and environmental factors. Environ Health Perspect. 2006; 114:165–72. [PubMed: 16451849]

Iga AM, Robertson JH, Winslet MC, Seifalian AM. Clinical potential of quantum dots. J Biomed Biotechnol. 2007; 2007:76087. [PubMed: 18317518]

Kobayashi H, Hama Y, Koyama Y, Barrett T, Regino CA, Urano Y, et al. Simultaneous multicolor imaging of five different lymphatic basins using quantum dots. Nano Lett. 2007a; 7:1711–6. [PubMed: 17530812]

Kobayashi H, Koyama Y, Barrett T, Hama Y, Regino ASC, Shin IS, et al. Multimodal nanoprobes for radionuclide and five-color nearinfrared optical lymphatic imaging. ACS Nano. 2007b; 1:258–64. [PubMed: 19079788]

Kobayashi H, Ogawa M, Kosaka N, Choyke PL, Urano Y. Simultaneous imaging of quantum dots-labeled cancer cell migration and lymphatic drainage using dendrimer-based optical agents. Nanomedicine. 2009 (in press).

Robe A, Pic E, Lassalle HP, Bezdetnaya L, Guillemin F, Marchal F. Quantum dots in axillary lymph node mapping: biodistribution study in healthy mice. BMC Cancer. 2008; 8:111. [PubMed: 18430208]

Sharma R, Wendt JA, Rasmussen JC, Adams KE, Marshall MV, Sevick-Muraca EM. New horizons for imaging lymphatic function. Ann N Y Acad Sci. 2008; 1131:13–36. [PubMed: 18519956]

Tanaka E, Choi HS, Fujii H, Bawendi MG, Frangioni JV. Image-guided oncologic surgery using invisible light: completed pre-clinical development for sentinel lymph node mapping. Ann Surg Oncol. 2006; 13:1671–81. [PubMed: 17009138]

Willard-Mack CL. Normal structure, function, and histology of lymph nodes. Toxicol Pathol. 2006; 34:409–24. [PubMed: 17067937]

Zhang T, Stilwell JL, Gerion D, Ding L, Elboudwarej O, Cooke PA, et al. Cellular effect of high doses of silica-coated quantum dot profiled with high throughput gene expression analysis and high content cellomics measurements. Nano Lett. 2006; 6:800–8. [PubMed: 16608287]

NIH-PA Author Manuscript

NIH-PA Author Manuscript

NIH-PA Author Manuscript

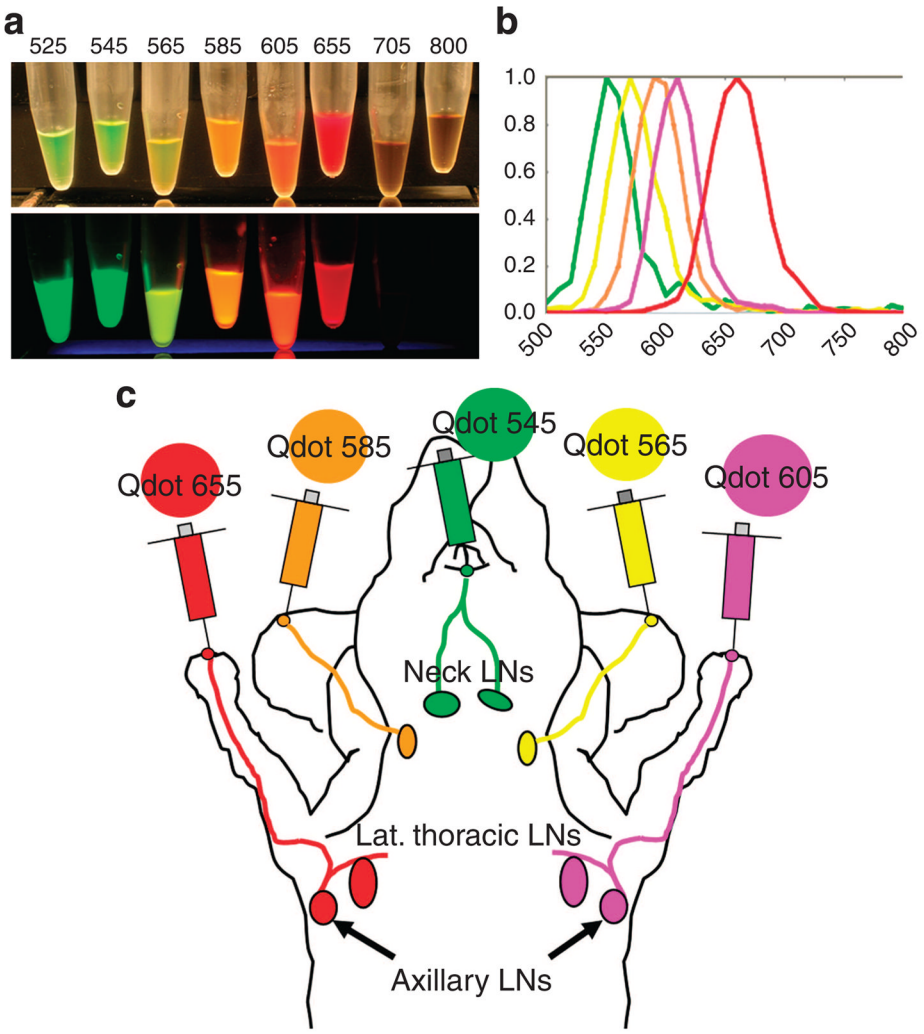

Figure 1. Selection of Qdots used in this study

(a) White-light image (upper) and fluorescence image (lower) of carboxyl quantum dots (From left to right; Qdots 525, 545, 565, 585, 605, 655, 705, and 800). Fluorescence image was excited by 365-nm ultra-violet light, and captured with a commercial-grade digital camera used in this study. Each visible-light Qdots show its distinct fluorescence, whereas two near-infrared Qdots (Qdot 705 and 800) are not visualized in the fluorescence image. (**b**) Graph of the emission spectra of each of the five carboxyl quantum dots used in this study (From left to right; Qdots 545, 565, 585, 605, and 655). (**c**) Schematic illustration of sites of injection in mice.

NIH-PA Author Manuscript

NIH-PA Author Manuscript

NIH-PA Author Manuscript

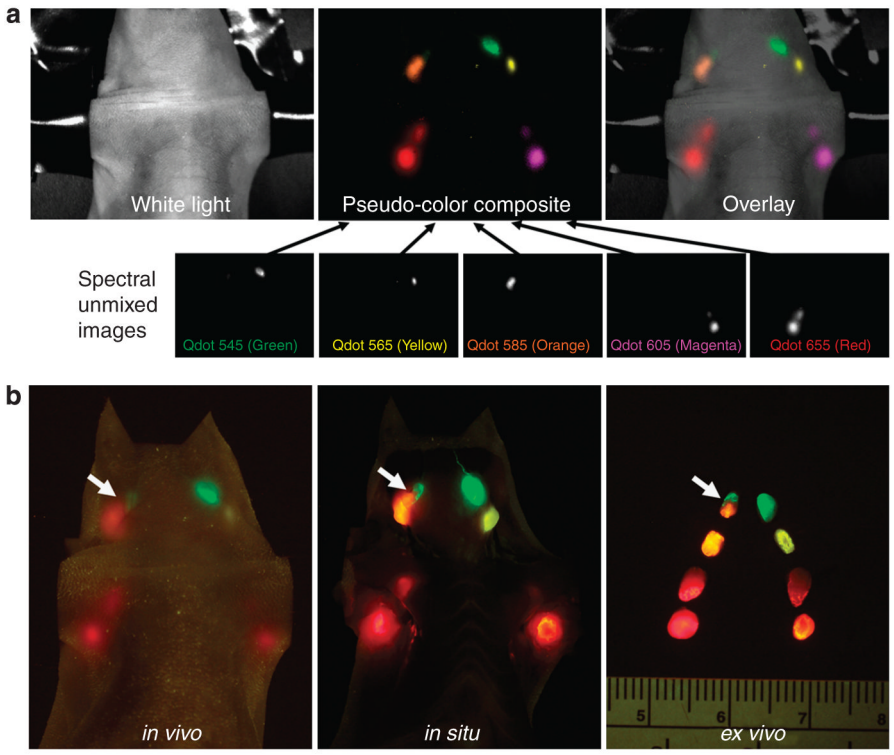

Figure 2. Multicolor fluorescence lymphatic images

(**a**) Spectral fluorescence imaging needs to create spectral unmixed images of each Qdot and then creates “pseudo-color” images to overlay on the white-light image. (**b**) Real-time fluorescence imaging does not require such post-processing, permitting real-time imaging. In this illustration a right superficial neck lymph node receives lymphatic drainage from two different lymphatic basins (arrows).

NIH-PA Author Manuscript

NIH-PA Author Manuscript

NIH-PA Author Manuscript

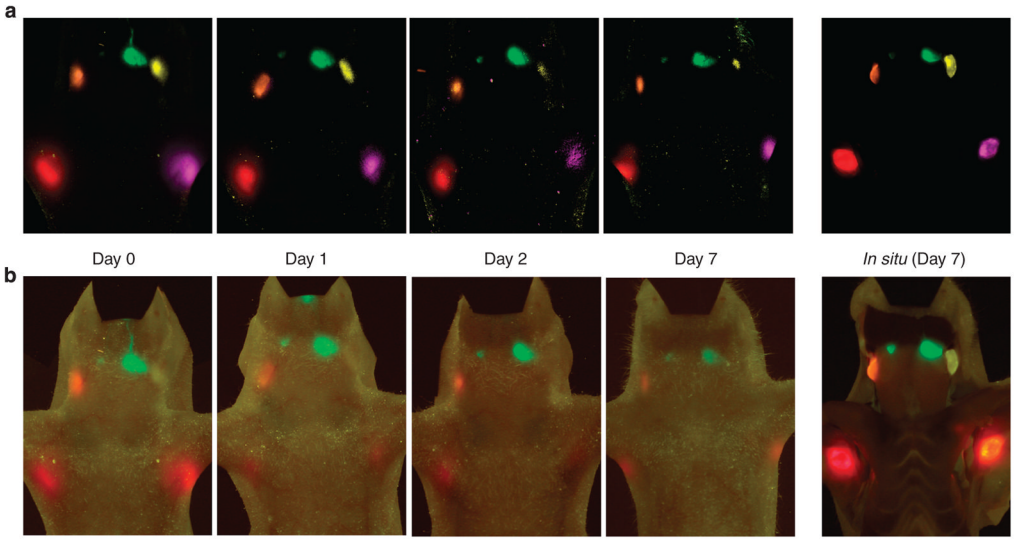

Figure 3. Serial *in vivo* fluorescence images at day 0 to day 7 and *in situ* fluorescence images at day 7

On day 1, signal is reduced compared to day 0. From day 1 to day 7, however, there are less marked reductions in signal, except in the left deep neck lymph node (Qdot 565), which becomes harder to see because of autofluorescence. *In situ* fluorescence images at day 7 clearly show all lymph nodes containing Qdots. (**a**) Spectral fluorescence images, (**b**) real-time multicolor fluorescence images.

NIH-PA Author Manuscript

NIH-PA Author Manuscript

NIH-PA Author Manuscript

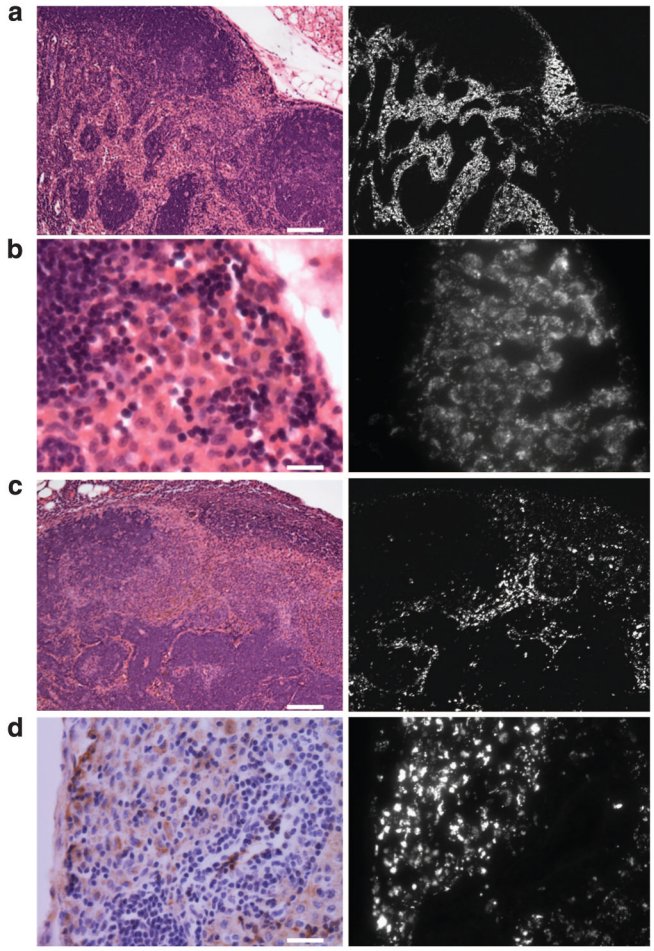

Figure 4. Intranodal localization of Qdots

Hematoxylin and eosin staining and fluorescence microscopic images of right axillary lymph nodes (containing Qdot 655) at day 0 (**a** and **b**) and day 7 (**c**). At day 0, Qdots mainly accumulated in the lymphatic sinuses, whereas lymphoid follicles and lymphatic cords were spared (**a**). The distribution of Qdots corresponds to the expected lymph fluid distribution within lymph nodes. At high magnification, the Qdots appear nodular with dark areas in the center rather than diffusely distributed (**b**), indicating that Qdots accumulate in the cytoplasm of cells within the lymphatic sinuses. After 7 days, the Qdot accumulation is sparser than on day 0, but is still nodular (**c**). HAM56 staining image is well correlated with the distribution of Qdots within macrophages and dendritic cells (**d**). Scale bars of **a**, **b**, **c**, and **d** = 100, 20, 100, and 25 μm, respectively.